E-ISSN: 2829-7687
Journal of Fibers and Polymer Composites
Vol. 5 No. 2 (2026): 177-194

Drying-Induced Hornification in Cellulose Nanofiber–PLA Composites Improving Mechanical and Thermal Stability

Sholahuddin Sholahuddin [a,*], Eka Fitriastuti [b], Dian Yosi Arinawati [c]

[a] Department of Agrotechnology, Faculty of Agriculture, Universitas Muhammadiyah Yogyakarta, Bantul, Indonesia
[b] Nusantara Scientific Research Center, Bantul, Indonesia
[c] Department of Oral Biology, Faculty of Dentistry, Universitas Muhammadiyah Yogyakarta, Bantul, Indonesia

Abstract. *Steam explosion pretreatment is widely used to facilitate the production of cellulose nanofibers (CNFs) from lignocellulosic biomass; however, the influence of pretreatment severity on the performance of CNF-reinforced polylactic acid (PLA) composites remains insufficiently understood. This study investigated the effect of steam explosion pressures of 35 and 40 atm on the mechanical, thermal, and morphological properties of CNF/PLA composites prepared from oil palm empty fruit bunches (EFB). CNFs were produced by steam explosion followed by mechanical fibrillation and incorporated into a PLA matrix at a 1:1 dry weight ratio. The composite prepared using 35 atm exhibited superior mechanical performance, with a tensile strength of 9.22 ± 0.01 MPa and a Young's modulus of 2.26 ± 0.12 GPa. Increasing the pretreatment pressure to 40 atm slightly delayed the onset of thermal degradation and reduced the cold crystallization temperature, suggesting enhanced heterogeneous nucleation during heating. However, the higher pressure also reduced tensile properties and significantly decreased the residual char content, indicating more extensive removal of lignin and possible hornification and partial cellulose depolymerization. These results demonstrate a trade-off between mechanical reinforcement and thermal performance as pretreatment severity increases. Overall, a steam explosion pressure of 35 atm provided the most balanced combination of mechanical and thermal properties, offering useful guidance for optimizing CNF-reinforced PLA biocomposites derived from oil palm biomass.*

Keywords: *Biorefinery; CNF/PLA composite; Hornification; biopolymer; oil palm empty fruit bunch.*

Type of the Paper: Regular Article.

1. Introduction

In recent years, there has been a growing demand for biodegradable packaging materials to replace conventional petroleum-based plastics, driven by environmental concerns and increasing regulatory pressure to reduce plastic waste. Polylactic acid (PLA), a bio-based and biodegradable thermoplastic, has been widely investigated and increasingly applied in packaging applications due to its renewability, good mechanical strength, processing versatility, and compostability [1] However, neat PLA films often exhibit limited barrier performance and relatively low thermal stability, which restricts their use in packaging applications that require robust protection and

https://doi.org/10.55043/jfpc.v5i2.587
Received March 10, 2026; Received in revised form July 9, 2026; Accepted July 11, 2026; Published July 31, 2026
* Corresponding author
Email: sholahuddin@umy.ac.id *

moderate temperature resistance [2]. To improve the above limitations, reinforcement of PLA with nanocellulose-based fillers such as Cellulose Nanofibers (CNF) has been identified as an effective approach for improving PLA-based materials, as nanocellulose materials possess high elastic modulus, high surface area, biodegradability, and gas barrier properties [3]. Previous studies have demonstrated that the incorporation of nanocellulose into PLA matrices has been shown to significantly improve the mechanical performance, barrier properties, and thermal stability, which are all important considerations in sustainable packaging materials [2]. Nanocellulose-reinforced PLA composites have been suggested to be used in sustainable packaging materials, which would extend the shelf life of products while at the same time reducing environmental impacts compared to traditional plastic packaging materials used in the packaging sector [4]. These materials would be important in packaging products within the agricultural sector, where biodegradability and durability are critical in reducing environmental impacts while at the same time improving sustainability within the supply chain.

Due to an increasing interest in sustainable material applications based on PLA, much effort has been put into studies about enhancing the mechanical and thermal properties of PLA through incorporating renewable nanofillers. One of the widely studied nanofillers includes cellulose nanofibers (CNFs) because of their outstanding mechanical properties, low density, aspect ratio, and high surface hydroxylic groups which lead to efficient reinforcement of PLA matrices [5,6]. The efficiency of CNFs in reinforcing of polymer matrix depends significantly on the level of CNFs' dispersion. Due to the phenomenon of hornification which takes place during drying, the number of accessible surface areas and binding sites decreases, leading to poor dispersion and weaker interactions between CNFs and PLA [7,8]. As the structure of CNFs is highly correlated with the process of preparation, specifically steam explosion, the optimization of steam explosion pressure can potentially affect hornification and hence the mechanical and thermal properties of the CNF/PLA composite.

Polylactic acid, also known as PLA, is an aliphatic polyester that is biodegradable, derived from renewable resources, and is considered an environmentally friendly substitute for conventional petroleum-based materials for the development of packaging materials, biomedical products, and environmental engineering. PLA is known for its good biodegradability and stiffness, but its poor thermal stability, low rate of crystallization, and brittleness restrict its use for other applications [4]. Therefore, the incorporation of nanomaterials, such as CNFs, is an important area of investigation for the better use of PLA. CNFs have high aspect ratios, high surface areas, and mechanical rigidity, which can improve the mechanical properties of the composite [9,10].

However, the hydrophilic nature of CNF and the hydrophobic nature of PLA pose problems of incompatibility at the interfaces, which are normally solved using techniques of surface modification and the addition of a compatibilizer, as in the traditional solution mixing technique. However, the presence of moisture or solvents, which are normally left in the composites after the traditional wet-blending and solution-casting techniques, has the potential to act as a catalyst in the hydrolytic degradation of PLA, thus reducing the molecular weight and the overall quality of the composites [11].

In this regard, the use of dry-state processing offers promise. This is because, in this method, the water content in the CNF is minimized before the mixture is blended with PLA in a thermomechanical environment. This will help in maintaining the integrity of the PLA chains. In earlier studies, it was established that the homogenous dispersion of the CNF in the PLA matrices is an essential factor in improving the mechanical and thermal properties of the materials. In this regard, the processing method is an important factor in determining the microstructure of the final product [10]. In the wet-state method, the wetting efficiency of the PLA in the porosity of the CNF is an added advantage.

The majority of the existing research studies on PLA/CNF composite materials have been based on solution casting, melt compounding, or wet-state mixing techniques, with emphasis given to the suppression of the agglomeration of CNF [12]. However, there is limited research attention given to the behavior of the composite system based on CNF and PLA in the dry state, especially when freeze-drying is used for the preservation of the composite structure. Freeze-drying is regarded as a less severe drying method when compared to oven drying, where the sublimation of ice is used to preserve the composite structure from the collapse of capillary forces. Nevertheless, the formation of ice crystals during the freezing step could induce the agglomeration of the composite material.

The ability to understand the influence of dried CNF on the crystallization and degradation of PLA is vital in development of packaging product that require thermal resistance during the manufacturing and storage phases. Differential Scanning Calorimetry (DSC) is instrumental in determining the glass transition temperature (T_g), cold crystallization temperature (T_{cc}), melting temperature (T_m), and the enthalpy associated with the crystallization of PLA. CNF is often used as a nucleating agent for PLA, resulting in faster crystallization rates [13]. The hornification of CNF, however, results in a reduction in the nucleation ability of the cellulose fibers. This means that the variation in Tg, Tcc, and the melting enthalpy (ΔHm) is an indication of the hornification intensity [14]. Thermogravimetric Analysis (TG) and Differential Thermal Analysis (DTA) provide additional information in support of DSC in the determination of the onset temperature of degradation (T5% or T_{onset}), the maximum degradation temperature (T_{max}), and the formation of

residue. The addition of CNF improves the thermal stability of the composite material by the barrier effect mechanism. Hornified CNF, which exhibits higher density of hydrogen bonding, has shown better thermal stability compared to the never-dried type of CNF. The reduction in low-temperature weight loss in the TG curve indicates the decrease in the amount of bound water, which is associated with the densification of the structure of the material during the drying process [15].

The mechanical characterization through tensile testing is vital to determine correlations between the microstructure and macroscopic properties. Cellulose nanofibers, if well dispersed, have been reported to improve substantially the modulus and strength of PLA-based composites by enabling stress transfer through the matrix-filler interface. Previous studies on PLA nanocomposites, which incorporated nanocellulosic materials, have proven that low loadings, ranging from 1 to 5 wt%, can improve significantly the elastic modulus, especially under processing conditions that favor the development of positive microstructures [16]. Tensile properties are also important evidence of the improvements in the structure of the composite material, which are the result of the application of certain processing techniques, such as vacuum mixing and freeze-drying.

Morphological analysis of the composite material is usually done using scanning electron microscopy (SEM). Uniform distribution of CNF and strong adhesion to PLA are indicators of an effective composite design, as agglomeration typically leads to stress concentration and early failure. Morphological observations in previous studies support the notion that microstructural uniformity is essential for synergistically enhancing the thermal and mechanical properties of PLA/CNF systems [16].

From an agricultural packaging perspective, moderate hornification may provide advantageous characteristics. Enhanced T_g and T_{onset} improve dimensional stability during storage under tropical climate conditions. Increased crystallinity may increase mechanical stiffness and reduce deformation. Moreover, the densified CNF network may improve oxygen barrier performance, extending the shelf life of agricultural products such as fresh produce and seeds [4]. However, excessive hornification could compromise flexibility and impact resistance, which are crucial for packaging durability during transportation. The present study investigates the fabrication of dry-state CNF/PLA composites prepared via vacuum-assisted planetary mixing followed by freeze drying. CNF (4% dry weight) was homogenized with liquid PLA under vacuum conditions to eliminate microbubbles and improve dispersion homogeneity before undergoing freeze drying. The mechanical properties were assessed through tensile testing, whereas thermal properties and hornification characteristics were investigated through DSC and TG/DTA analyses, respectively. The morphological properties were investigated through characterization.

In contrast to previous research works that mainly dealt with optimization of PLA composites by means of addition of fillers and/or modification of their surface, this work is devoted to the role of the production history of the cellulose nanofibers (CNFs) on the properties of the corresponding composites. In particular, different variants of CNFs obtained at various steam explosion pressures were examined for the study of the impact of differences in the pretreatment regime on the hornification of the CNFs during the drying process, further CNF dispersion in the PLA matrix, and thermo-mechanical properties of the composites. The freeze-drying process was used to retain the structure of CNFs before composite preparation, while vacuum-assisted planetary mixing was used for dry dispersion of CNFs in the PLA matrix. Thus, this study elucidates the processing–structure–property relationships in the biorefinery conversion of oil palm empty fruit bunches into CNF/PLA biocomposites by correlating steam explosion pretreatment severity with hornification, CNF structure, dispersion within the PLA matrix, and the resulting mechanical and thermal properties.

2. Materials and methods

2.1. CNF Preparation

Cellulose nanofiber was prepared used palm oil empty fruit bunches (POEFB) pretreated with steam explosion. The POEFB was chopped into 3-5 cm and oven dried in 60 °C for 24 hours with 14% moisture content. The oven dried POEFB (200 gr without mixed with water) continue to steam explosion pretreatment. The steam explosion was conducted using a 2-L reactor (NK-2L, Japan Chemical Engineering and Machinery Co. Ltd., Osaka, Japan) regulated by deionized water in condition at 35 and 40 ATM for 5 minutes. The severity factor (R_0) from the steam explosion pretreatment was calculated using the following Formula (1).

$$R0 = t.\exp[(Tr - 100)/14.75] \quad (1)$$

Tr is the temperature reaction (°C), and *t* is the resident time [17]. The severity factors for 35/5 and 40/5, were 4.91, and 5.12. Steam-exploded POEFB continued to extraction process following the method Sholahuddin [10]. The CNF than continue to centrifuge process at 2.000 RPM for 15 minutes to get 4% DW and storage it in sealed bottle at 4°C.

2.2. Dried-state CNF/PLA composite

The dry-state CNF/PLA composite was prepared by mixing cellulose nanofibers (CNFs) and liquid PLA at a 1:1 ratio on a dry-weight basis, corresponding to a final CNF loading of 50 wt% in the composite. Liquid PLA (Landy P1000, Miyoshi Oil & FAT Co., Ltd.) was used as the polymer matrix. The CNF and PLA were mixed using a pressurized planetary mixer (Thinky ARV-310P) in two stages. The first stage was performed at 1,500 rpm under atmospheric pressure for 5

min, followed by a second stage at 2,000 rpm under 5 Torr for 15 min to remove entrapped air bubbles and improve dispersion. The resulting composite was frozen at −80 °C for 24 h in a sealed container and subsequently freeze-dried at −50 °C. After freeze-drying, the composite was ground into a fine powder and further dried in a vacuum oven at 40 °C for 24 h to reduce the residual moisture content to below 0.5 wt%. The dried composite powder was stored in a desiccator until moulding to prevent moisture uptake

2.3. Mechanical properties

The tensile test was evaluate use moulded CNF-PLA composite. The specimens were prepared with identical dimensions (100 mm × 10 mm × ±0.1 mm) and tested in triplicate, used metal mould. The metal mould was heated at 45 °C before the CNF/PLA added into the mould. The mould set at 110 °C continue to pressed (3 MPa) for 30 minutes. The Young's modulus, tensile strength, and elongation at break were determined using a universal testing machine at ambient temperature. The crosshead speed was maintained at 1.0 mm/min. All specimens were prepared with identical dimensions (100 mm × 10 mm × ±0.1 mm) and tested in triplicate. The gauge length for each measurement was fixed at 30 mm.

2.4. Morphological evaluation

The dried-state CNF/PLA composite powder continue to morphological examination to confirm the CNF and PLA bonding during the dried-state by used scanning electron microscope (JEOL JCM-6000Plus). Prior to observation, the freeze-dried CNF/PLA composite samples were sputter-coated with platinum using an auto fine coater under air purge conditions. The SEM analysis was conducted under high vacuum at an accelerating voltage of 15 kV with a standard filament. Micrographs were captured at a magnification of 3000× (43 mm) with a 10 µm scale bar.

2.5. Thermal properties

2.5.1. Differential Scanning Calorimetry (DSC)

The dried-state CNF/PLA composite powder continues to thermal characterization using differential scanning calorimetry (DSC). The DSC (Exstar 6000; Seiko Instruments Inc.) was used to measure the glass transition temperature (Tg), thermal analysis was conducted on 5–5.5 mg CNF/PLA composite powder. The DSC was set at 30–550 °C with 20 °C/min temperature flow and injecting nitrogen at 50 mL/min.

2.5.2. Thermogravimetric Analysis (TG)

The percentage weight loss of LML was determined by thermogravimetric analysis (TG) using a thermogravimetric analyzer (TG/DTA SII EXSTAR6300, Seiko Instruments Inc.). Measurements were performed over a temperature range of 20–800 °C at a heating rate of 5 °C/min under a continuous nitrogen flow of 200 mL/min. The limiting oxygen index (LOI) of the specimens was evaluated according to ASTM D2863. The starting tem- perature of losing mass

(Ts), which is used to identify the temperature at which the samples start losing mass, was defined from the weight loss temperatures at 5% and 30% using the following equation.

Degradation properties of CNF/PLA composites were characterized using TGA through a thermogravimetric analyzer (TG/DTA SII EXSTAR6300, Seiko Instruments Inc.). Experiments were performed in the temperature range of 20-800°C with a heating rate of 5°C min^{-1} in a constant nitrogen atmosphere with a nitrogen flow rate of 200 mL min^{-1}. Onset degradation temperatures (T5% and T30%) were obtained based on the temperature value when the samples lost 5% and 30% weight, respectively, according to the following Formula (2).

$$Ts = 0.49[Td5 + 0.6(Td30 - Td5)] \quad (1)$$

3. Results and Discussion

3.1 Morphological

The micrograph (Fig. 1) of CNF from EFB obtained at 35 atm (A) reveals a well-fibrillated network structure composed of entangled nanofibers with relatively uniform diameters. The fibrils appear individualized and form an interconnected web-like morphology Steam explosion pretreatment effectively removes amorphous components such as hemicellulose and lignin while exposing cellulose microfibrils and facilitating fibrillation [1]. The nanofibers are still of sufficient length and aspect ratio, which are vital parameters in stress transfer in composite systems. Some level of aggregation is also observed, indicating the potential for dispersibility in the melt blending with PLA. For the higher severity in 40 atm, the CNF from EFB, as in morphology B, exhibits a level of structural densification and aggregation. While there is still some level of fibrillation, the CNF is now more compact and exhibits some level of bundling. CNF obtained from EFB is known to have a nanoscale fibrillar structure with interconnected network morphology, which is beneficial in reinforcement applications [18]. The level of compactness and aggregation is observed, and this could be attributed to the hornification effect, which is a phenomenon arising due to the formation of irreversible hydrogen bonds between the adjacent fibrils [19]. The level of compactness also indicates a higher level of purification and crystallinity, but the level of aggregation could affect the level of surface area and the potential for redisperseability. Aggregation could also affect the level of CNF dispersibility and the interfacial effect in PLA-based CNF nanocomposites [13].

Dried composite EFB prepared using the CNF/PLA from 35 atm (C) displays relatively uniform particle dispersion. The morphology displays fine and rounded domains with minimal agglomeration, indicating the efficient dispersion of the nanofibers in the PLA matrix. The absence of large agglomerates indicates the strong interfacial compatibility and stress transfer ability. Uniform dispersion has been reported to improve the stress transfer efficiency, resulting in improved tensile strength and modulus in PLA nanocomposites [20]. This level of microstructural

uniformity is also associated with the increased tensile strength and modulus observed in the mechanical tests. In contrast, it is seen that, for the dried composite containing CNF/PLA at 40 atm, D, there is greater agglomerate and cluster formation. Larger spherical domains and aggregates can be seen, suggesting that the level of dispersion is less effective. The agglomerated fibril bundles will be acting as micro-scale fillers, as opposed to reinforcement at the nanoscale. This is related to the higher variability and slightly reduced tensile properties recorded for this composite. This is attributed to the fact that the aggregated nanofiber bundles could act as micro-scale filler materials, leading to stress concentration in the material [21].

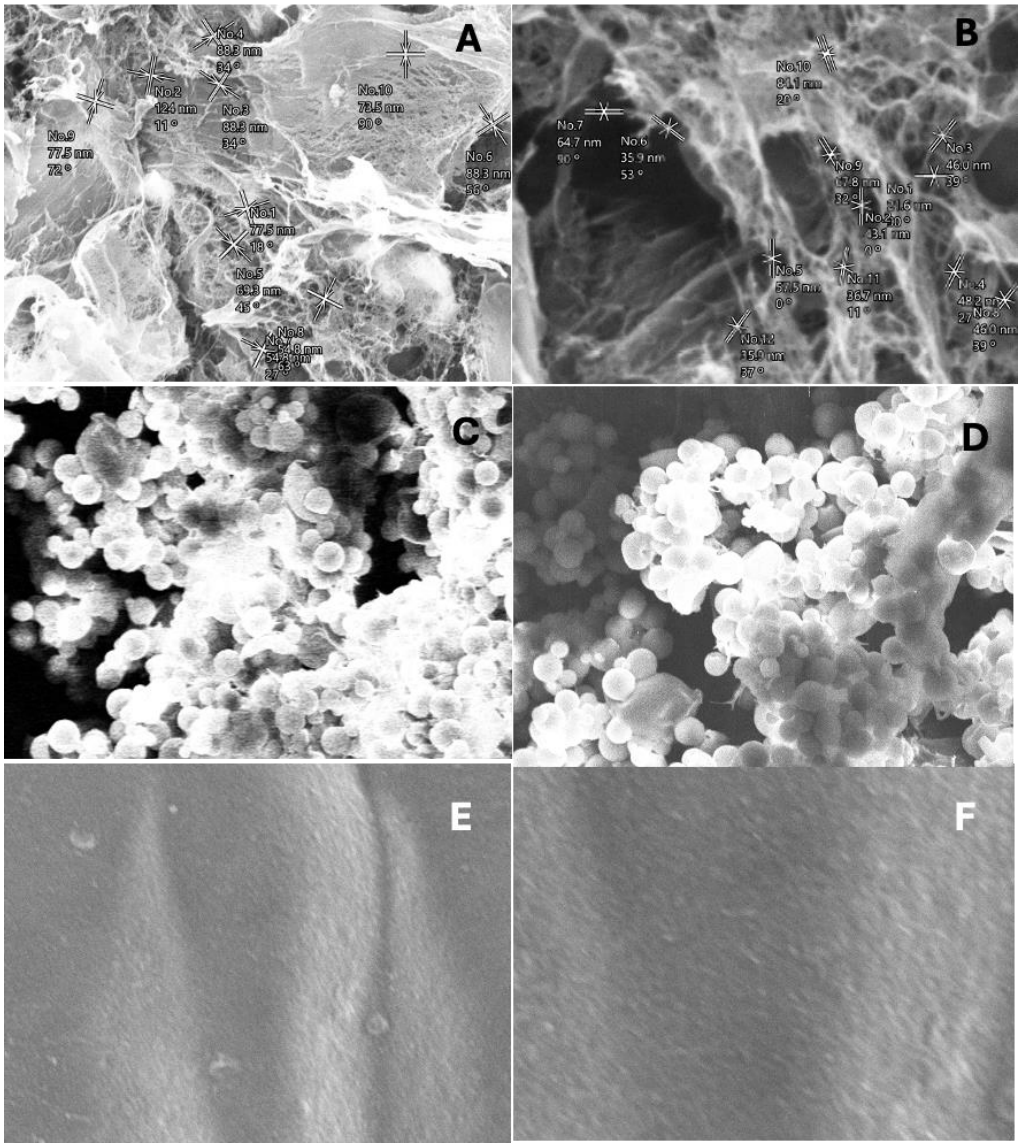

Fig. 1. The CNF from EFB 35 (A), CNF from EFB 40 (B), dried CNF/PLA composite EFB 35 (C), dried CNF/PLA composite EFB 40 (D), surface morphological of moulded CNF/PLA composite EFB 35 (E), surface morphological of moulded CNF/PLA composite EFB 40 (F).

The moulded surface morphology of the moulded CNF/PLA composite of the 35 atm (E) composite is observed to have a good surface texture, which is smooth and continuous with minor irregularities on the surface. Such surface texture is an indication of good melt flow behavior and

good interfacial adhesion between the nanofibers and the PLA matrix [22]. The lack of large voids or pull-out marks indicates the high level of adhesion between the interfaces and the cohesive nature of the structural integration. The surface morphology of the moulded surface of the composite material of the 40 atm (F) composite, comprising moulded CNF/PLA, presents a slightly rougher surface texture with micro-heterogeneity features. The micro-scale surface features could be attributed to the presence of aggregated domains of the nanofiber reinforcement or the lack of interfacial bonding between the reinforcement and the polymer matrix. The surface roughness is often linked to the aggregation of the nanofiber reinforcement within the polymer matrix [23]. This surface irregularity is a consequence of less uniform stress transfer in the moulding process and mechanical loading. In spite of the improvement in thermal resistance, the microstructure's compactness and fibril aggregation are thought to hinder the reinforcement efficiency. This is because the aggregated bundles of nanofibers are more likely to behave as microscale reinforcements, thus resulting in less efficient stress transfer [24].

3.2 Mechanical character

The tensile properties of CNF/PLA composites also clearly reflect the effect of severity of steam explosion process on reinforcement efficiency and structural integrity of cellulose nanofibers. Quantitative mechanical parameters clearly show that there is a decrease in strength and stiffness with an increase in severity from 35 atm to 40 atm. The CNF/PLA EFB 35 composite material has a maximum test force (Fm) of 105.34 ± 0.84 N, which is significantly higher than the CNF/PLA EFB 40, with a maximum test force (Fm) of 95.36 ± 3.69 N. The low standard deviation of the CNF/PLA EFB 35 composite materials indicates the efficient distribution of stress and uniformity in the composite matrix. However, the high standard deviation of the CNF/PLA EFB 40 composite materials indicates the variation in the uniformity of the composite materials, which could have been caused by the aggregation and degradation of the CNF structures during the steam explosion pretreatment at higher severity, i.e., 40 atm. The same trend is observed for the maximum stress point (Rm). The decrease in tensile strength is found to be in the range of 9.22 ± 0.01 MPa for EFB to 8.25 ± 0.92 MPa to EFB 40. Though the decrease in the values may be found to be moderate, the increase in the values of deviation may be due to the unstable behavior of reinforcement. The decrease in the values of tensile strength may be due to the increase in the pretreatment severity. Steam explosion at high pressure may cause the depolymerization of the cellulose chains. This may cause a decrease in the strength of the fibers as the chains are shorter in size and may be unable to carry the stress effectively in the PLA matrix [25,26].

Table 1. Mechanical properties of CNF/PLA composites (Mpa and GPa).

Sample	Maximum test force (F_m) N	Maximum stress point (R_m) Mpa	Young's Modulus Gpa
CNF/PLA EFB 35	105.34 ±0.84	9.22 ±0.01	2.26 ±0.12
CNF/PLA EFB 40	95.36 ±3.69	8.25 ±0.92	2.16 ±0.17

Young's modulus also supports this interpretation, as it reduces from 2.26 ± 0.12 GPa for EFB 35 to 2.16 ± 0.17 GPa for EFB 40. The change is not dramatic but does reflect a decrease in stiffness as severity of treatment increases. For nanocomposite systems, an enhancement in stiffness is generally achieved by high aspect ratio fillers and high adhesion between fillers and matrix. For nanocomposite systems, an enhancement in stiffness is generally achieved by high aspect ratio fillers and high adhesion between fillers and matrix [24]. If the severity of steam explosion is too high, two counteractive processes can happen simultaneously: an increase in the degree of crystallinity of cellulose, which enhances rigidity, and an increase in hornification or fibril aggregation, which reduces the effective surface area for redisperseability of nanofibers, thus affecting bonding efficiency with PLA. The mechanical properties, therefore, show a trade-off. The 35 atm condition seems to offer the best compromise for lignin removal, fibrillation, and the integrity of the cellulose backbone. The nanofibers have adequate length and aspect ratio to create an efficient reinforcing network in the polymer matrix. Good stress transfer is possible through adequate dispersion and interface interaction. However, at 40 atm, the higher severity not only improves purification and ordering but could also enhance the formation of irreversible hydrogen bonding between adjacent cellulose fibrils, a process known as hornification. It is the formation of irreversible hydrogen bonding between adjacent fibrils, which causes a reduction in the surface area and redisperseability of the nanofibers [23]. This densification also affects the flexibility and redisperseability of the nanofibers during the melt processing step in combination with PLA. The fibril aggregates behave like micro-scale fillers rather than nanoscale reinforcements, which results in a decrease in the stress transfer efficiency. Moreover, the possibility of chain scission during the high-pressure steam treatment also affects the degree of polymerization, which in turn affects the intrinsic tensile strength of the fibers. Moreover, the high hydrothermal treatment also leads to the depolymerization of the cellulose chains, which affects the intrinsic strength of the fibers [27]. Interestingly, the mechanical reduction occurs simultaneously with the enhancement of thermal stability, as measured by Td5 and Ts. This suggests that thermal resistance and tensile reinforcement do not scale linearly. The enhancement of thermal stability is due to increased crystallinity and structural densification, whereas the enhancement of tensile performance is critically dependent on the structural integrity of the fibers, aspect ratio, and homogeneous dispersion.

Furthermore, Young's modulus is consistent with the above explanation, as it decreases from 2.26 ± 0.12 GPa for EFB 35 to 2.16 ± 0.17 GPa for EFB 40, which shows that the stiffness of the material decreases with increased severity of steam explosion treatment. In the case of CNF-reinforced composites, stiffness depends on such parameters as the aspect ratio of nanofibers, their distribution inside the polymer matrix, and the quality of the fiber-matrix interface [24]. The improved mechanical properties of the EFB 35 composite demonstrate that such conditions of steam explosion treatment are optimal, because they allow removing excess lignin, making cellulose fibers fibrillated, while not damaging their structure to efficiently transfer stresses inside the PLA matrix. At the same time, increased pressure during steam explosion (40 atm) leads to hornification caused by drying, which results in irreversibly formed CNF aggregates that have decreased surface area and redispersibility [23]. The higher steam explosion intensity may cause partial degradation of the cellulose structure and thereby contribute to the decrease in tensile properties observed [27]. Even though the 40 atm steam explosion improved the initial thermal stability of the composites, the decrease in the tensile strength and Young's modulus suggests a tradeoff between the thermal stability and the mechanical reinforcement of the composites.

On the whole, as shown by the mechanical analysis, moderate steam explosion severity, that is, 35 atm, results in better efficiency of reinforcement, as indicated by higher values of Fm, that is, 105.34 N, tensile strength, that is, 9.22 MPa, and Young's modulus, that is, 2.26 GPa. Increasing the severity to 40 atm indicates a shift towards increased rigidity of the composite material while slightly compromising its mechanical properties due to hornification and possible depolymerization [28]. The results obtained in this study show that optimal pretreatment conditions must provide a balance between purification, fibrillation, and preservation of integrity of molecules. Severe steam explosion may improve thermal resistance but reduce mechanical reinforcement efficiency. Therefore, steam explosion parameters play a critical role in developing CNF/PLA biocomposites with enhanced [29].

3.3 Thermal character

3.3.1 Differential Scanning Calorimetry

Using the Differential Scanning Calorimetry method, significant differences are observed in the glass transition and cold crystallization temperature crystallization of the composites. A distinct melting peak was not observed during the first heating scan. The DSC analysis was performed using a single-heating program up to high temperature, and the thermal decomposition event overlapped with the melting region. Consequently, the high-temperature peak observed at approximately 360 °C was assigned to thermal decomposition rather than the melting transition of PLA. The glass transition temperature (T_g) of the composites decreased from 59.21°C (35 atm) to 52.77°C (40 atm). The T_g value decreased due to the increased chain mobility of PLA in the

amorphous region as a result of the increased pretreatment severity. The purification of cellulose increased at 40 atm; however, hornification may have reduced the interaction between the polymers and the nanofibers. The presence of aggregated fibrils caused a reduction in the molecular restriction of PLA chains, resulting in a lower T_g value [16]. It has been widely reported that cellulose nanofibers act as heterogeneous nucleating agents for PLA crystallization [30]. n the present study, the cold crystallization temperature (Tcc) decreased significantly from 100.47 °C for the CNF/PLA EFB 35 composite to 89.14 °C for the CNF/PLA EFB 40 composite. This reduction indicates that crystallization occurred at a lower temperature, suggesting that the CNFs produced under the higher steam explosion pressure provided more effective heterogeneous nucleation sites for PLA crystallization. Similar nucleation behavior has been reported for PLA composites containing silica/lignin hybrid fillers, where the incorporation of fillers promoted cold crystallization and enhanced the nucleation capability of the PLA matrix [31]. Meanwhile, the decrease in Tg indicates increased molecular chain mobility in the amorphous region. These thermal characteristics are consistent with the mechanical results, which showed a reduction in the reinforcement efficiency of the CNF/PLA composites.

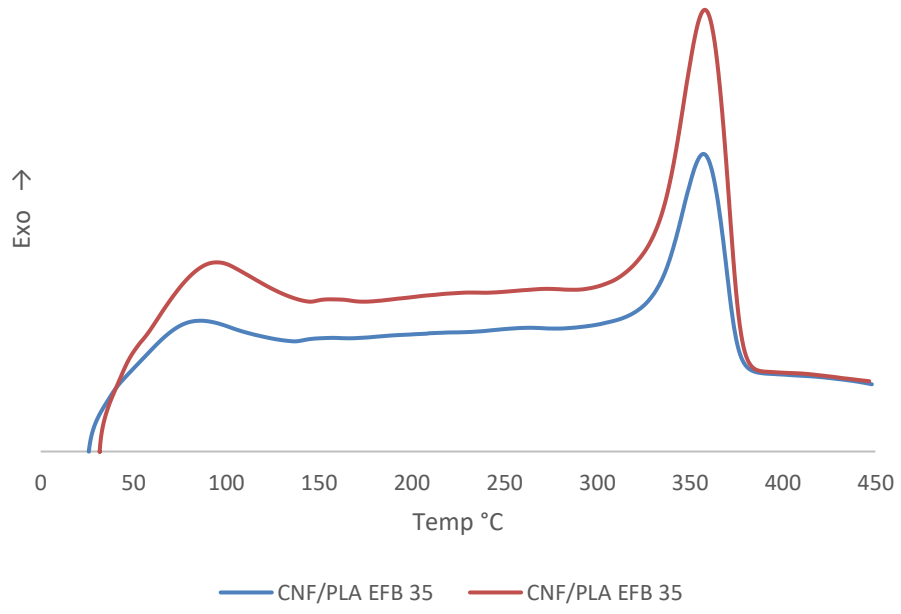

Fig. 2. DSC curve of CNF/PLA composite powder

3.3.2 Thermogravimetric Analysis

Thermogravimetric analysis (TGA) revealed the effect of steam explosion severity on the thermal degradation behavior of the CNF/PLA composites. The initial degradation temperatures (Td_5) of the CNF/PLA EFB 35 and CNF/PLA EFB 40 composites were nearly identical, at 244.61 °C and 244.69 °C, respectively. Although the increase was marginal, the slightly higher Td_5 of the EFB 40 composite indicates that the onset of thermal degradation was slightly delayed, suggesting a modest improvement in the initial thermal resistance of the composite. This behavior is likely associated with the removal of thermally unstable non-cellulosic components during the more severe steam explosion pretreatment. At Td_{10}, the EFB 35 and EFB 40 composites exhibited values of 267.62 °C and 264.99 °C, respectively, while Td_{30} decreased from 301.54 °C to 297.59 °C. These results indicate that although the initial degradation behavior remains comparable, the thermal stability during the intermediate degradation stage slightly decreased in the EFB 40 composite. This reduction may be attributed to the partial depolymerization of cellulose caused by the higher steam explosion severity, producing cellulose chains with lower molecular weight that decompose more readily once thermal degradation has commenced [32].

The maximum degradation temperature (Tmax), determined from the DTG peak, was 316.53 °C for the CNF/PLA EFB 35 composite and 316.66 °C for the CNF/PLA EFB 40 composite. The nearly identical Tmax values indicate that increasing the steam explosion pressure from 35 to 40 atm had no significant influence on the principal thermal degradation mechanism of the PLA/CNF composites [33]. A pronounced difference was observed in the residual char content. The residue decreased markedly from 2.90% for the CNF/PLA EFB 35 composite to 0.08% for the CNF/PLA EFB 40 composite. The substantially lower char residue suggests that the more severe pretreatment effectively removed lignin and other aromatic constituents, thereby reducing the carbonization capability of the composite during pyrolysis [34,35]. Because lignin is the primary precursor for char formation, the near-zero residue observed in the EFB 40 composite indicates a highly purified cellulose structure with a reduced aromatic fraction. The onset temperature of mass loss (Ts) increased slightly from 136.59 °C to 139.43 °C, indicating a minor improvement in the initial thermal stability of the composite. This slight increase may reflect stronger intermolecular interactions and a more compact composite structure resulting from the higher steam explosion severity [36].

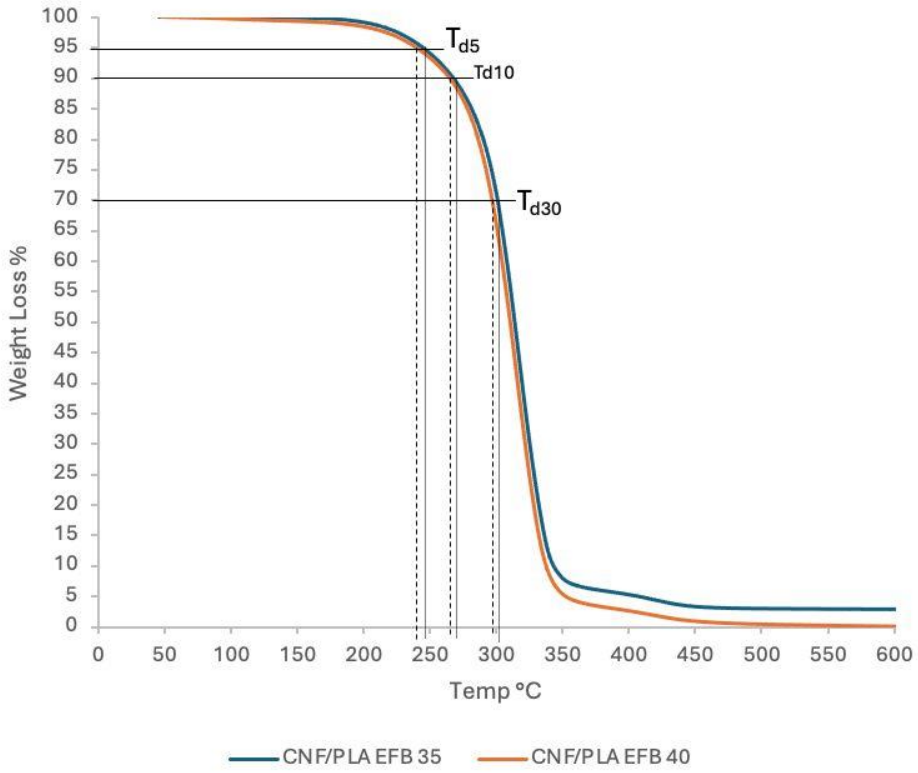

Fig. 3. TG curve of CNF/PLA composite powder

Table 2. Thermal characteristics of CNF/PLA composite powders

Sample	Td5 (°C)	Td10 (°C)	Td30 (°C)	Tmax (°C)	Residue (%)	Ts (°C)	Tg (°C)	Tcc (°C)
CNF/PLA EFB 35	244.61	267.62	301.54	316.53	2.90	136.59	59.21	100.47
CNF/PLA EFB 40	244.69	264.99	297.59	316.66	0.08	139.43	52.77	89.14

Overall, increasing the steam explosion pressure from **35 atm to 40 atm** produced only a marginal increase in the onset of thermal degradation, while slightly reducing the thermal stability during the intermediate degradation stage. The unchanged Tmax indicates that the fundamental degradation mechanism remained unaffected by the pretreatment severity. Conversely, the significant reduction in char residue demonstrates that the higher pretreatment severity effectively removed lignin, resulting in a purified cellulose structure with reduced carbonization capability. These thermal characteristics are consistent with the mechanical results, which showed a slight reduction in reinforcement efficiency for the EFB 40 composite, indicating a trade-off between cellulose purification and composite performance. A significant decrease in the amount of residual char is observed from 2.90% to 0.08%, implying a reduced lignin component and a corresponding reduced capacity for carbonization [9]. Therefore, at 40 atm pretreatment condition results in a composite system that is more rigid, purified, and has a later onset of degradation, along with enhanced molecular restriction [37]. Nevertheless, this improvement in the rigidity of the

composite material is accompanied by a decrease in the amount of char formed and a slight reduction in the material's tensile strength. This implies a trade-off effect [38]. This shows that the 35 atm condition presents a balance of mechanical properties and high-temperature carbon stability, while the 40 atm condition presents enhanced thermal resistance/rigidity at the early degradation stage. The selection of the pretreatment condition should be dependent on the desired end-use of the material.

4. Conclusions

This study demonstrates that steam explosion pressure plays a critical role in determining the processing–structure–property relationships of CNF/PLA composites derived from oil palm empty fruit bunches. A pretreatment pressure of 35 atm provided the optimum balance between cellulose fibrillation and structural integrity, resulting in superior mechanical performance, while increasing the pressure to 40 atm slightly delayed the onset of thermal degradation and promoted cold crystallization but reduced tensile properties and char residue due to increased cellulose purification, hornification, and partial cellulose depolymerization. These findings highlight a trade-off between thermal stability and mechanical reinforcement, indicating that excessive pretreatment severity does not necessarily improve the overall performance of CNF/PLA composites. However, this study was limited to the evaluation of mechanical, thermal, and morphological properties. Future work should include barrier properties, biodegradability, migration behavior, packaging performance, and comparison with neat PLA to comprehensively assess the potential of these biocomposites for sustainable biodegradable packaging applications.

Data availability statement

Data will be made available on request.

CRediT authorship contribution statement

Sholahuddin Sholahuddin: Conceptualization, Methodology, Data curation, Formal analysis, Funding acquisition, Investigation, Resources, Validation, Visualization, Writing – original draft, Writing-review, editing; **Eka Fitriastuti**: Resources, Visualization, templating; **Dian Yosi Arinawati**: Resources, Validation, Writing – original draft, Writing – review and editing.

Declaration of Competing Interest

The authors declare that they have no known competing financial interests or personal relationships that could have appeared to influence the work reported in this paper.

Acknowledgement

The authors would like to express our sincere gratitude to Prof. Yoshitoshi Nakamura and Prof. Chikako Asada for providing access to the steam explosion apparatus at the C3 Laboratory,

Tokushima University. This research was supported in part by Research Grant No. 11202310 from the Nusantara Scientific Research Center (NSRC), Indonesia, and by an internal research grant from the Muhammadiyah University Yogyakarta, Indonesia.

References

[1] Rajendran DS, Venkataraman S, Jha SK, Chakrabarty D, Kumar VV. A review on bio-based polymer polylactic acid potential on sustainable food packaging. Food Sci Biotechnol 2024;33:1759–88. https://doi.org/10.1007/s10068-024-01543-x.

[2] Domenek S, Louaifi A, Guinault A, Baumberger S. Potential of Lignins as Antioxidant Additive in Active Biodegradable Packaging Materials. J Polym Environ 2013;21:692–701. https://doi.org/10.1007/s10924-013-0570-6.

[3] Mosab Kaseem, Zeeshan Ur Rehman SH, Dikici AKS and B. A Review on Synthesis, Properties, and Applications of Polylactic Acid/Silica Composite. Lecture Notes in Mechanical Engineering 2024:703–20. https://doi.org/10.1007/978-981-97-3173-2_49.

[4] Asada C, Sholahuddin, Nakamura Y. Lignin as a Coating and Curing Agent on Biodegradable Epoxy Resins. In: Gutiérrez TJ, editor. Reactive and Functional Polymers Volume One, Springer International Publishing; 2020, p. 195–206. https://doi.org/10.1007/978-3-030-43403-8_9.

[5] Gray D. Nanocellulose: From Nature to High Performance Tailored Material 2013;67:353. https://doi.org/10.1515/hf-2013-0027.

[6] Klemm D, Kramer F, Moritz S, Lindström T, Ankerfors M, Gray D, et al. Nanocelluloses: A New Family of Nature-Based Materials. Angew Chem Int Ed 2011;50:5438–66. https://doi.org/10.1002/anie.201001273.

[7] Fernandes Diniz JMB, Gil MH, Castro J. Hornification—its origin and interpretation in wood pulps. Wood Sci Technol 2004;37:489–94.

[8] Hubbe MA, Rojas OJ, Lucia LA. Green Modification of Surface Characteristics of Cellulosic Materials at the Molecular or Nano Scale: A Review. Bioresources 2015;10.

[9] Asada C, Sholahuddin, Nakamura Y. Biorefinery System of Lignocellulosic Biomass Using Steam Explosion. In: Sand A, Banga S, editors. Cellulose Science and Derivatives, London: intechOpen; 2021, p. 73–98. https://doi.org/10.5772/intechopen.98544.

[10] Sholahuddin S, Arinawati DY, Setiawan CK, Utama NA, Prabasari I, Budiyanto G, et al. Characterization of Cellulose Nanofiber (CNF) from Steam-exploded Palm Oil Kernel Fibers Followed by Supermasscolloider. IOP Conf Ser Earth Environ Sci 2024;1417. https://doi.org/10.1088/1755-1315/1417/1/012038.

[11] Asada C, Honjo K, Nakamura Y. Utilization of Steam-Treated and Milling-Treated Lignin from Moso Bamboo as Curing Agent of Epoxy Resin. Waste Biomass Valorization 2021;12:6261–72. https://doi.org/10.1007/s12649-021-01444-8.

[12] Özdemir B, Nofar M. Effect of solvent type on the dispersion quality of spray-and freeze-dried CNCs in PLA through rheological analysis. Carbohydr Polym 2021;268. https://doi.org/10.1016/j.carbpol.2021.118243.

[13] Shazleen SS, Yasim-Anuar TAT, Ibrahim NA, Hassan MA, Ariffin H. Functionality of cellulose nanofiber as bio-based nucleating agent and nano-reinforcement material to enhance crystallization and mechanical properties of polylactic acid nanocomposite. Polymers (Basel) 2021;13:1–19. https://doi.org/10.3390/polym13030389.

[14] Ding Q, Zeng J, Wang B, Tang D, Chen K, Gao W. Effect of nanocellulose fiber hornification on water fraction characteristics and hydroxyl accessibility during dehydration. Carbohydr Polym 2019;207:44–51. https://doi.org/10.1016/j.carbpol.2018.11.075.

[15] Dufresne A. Nanocellulose: A new ageless bionanomaterial. Materials Today 2013;16:220–7. https://doi.org/10.1016/j.mattod.2013.06.004.

[16] Jonoobi M, Harun J, Mathew AP, Oksman K. Mechanical properties of cellulose nanofiber

(CNF) reinforced polylactic acid (PLA) prepared by twin screw extrusion. Compos Sci Technol 2010;70:1742–7. https://doi.org/10.1016/j.compscitech.2010.07.005.
[17] Overend RP, Chornet E, Gascoigne JA. Fractionation of Lignocellulosics by Steam-Aqueous Pretreatments [and Discussion]. Philosophical Transactions of the Royal Society of London Series A, Mathematical and Physical Sciences 1987;321:523–36.
[18] Gea S, Siregar AH, Zaidar E, Harahap M, Indrawan DP, Perangin-Angin YA. Isolation and characterisation of cellulose nanofibre and lignin from oil palm empty fruit bunches. Materials 2020;13. https://doi.org/10.3390/ma13102290.
[19] Spence KL, Venditti RA, Rojas OJ, Habibi Y, Pawlak JJ. A comparative study of energy consumption and physical properties of microfibrillated cellulose produced by different processing methods. Cellulose 2011;18:1097–111. https://doi.org/10.1007/s10570-011-9533-z.
[20] Iyer KA, Torkelson JM. Green composites of polypropylene and eggshell: Effective biofiller size reduction and dispersion by single-step processing with solid-state shear pulverization. Compos Sci Technol 2014;102:152–60. https://doi.org/10.1016/j.compscitech.2014.07.029.
[21] Le Duigou A, Davies P, Baley C. Macroscopic analysis of interfacial properties of flax/PLLA biocomposites. Compos Sci Technol 2010;70:1612–20. https://doi.org/10.1016/j.compscitech.2010.06.001.
[22] Hollingbery LA, Hull TR. The fire retardant effects of huntite in natural mixtures with hydromagnesite. Polym Degrad Stab 2012;97:504–12. https://doi.org/10.1016/j.polymdegradstab.2012.01.024.
[23] Lee KY, Aitomäki Y, Berglund LA, Oksman K, Bismarck A. On the use of nanocellulose as reinforcement in polymer matrix composites. Compos Sci Technol 2014;105:15–27. https://doi.org/10.1016/j.compscitech.2014.08.032.
[24] Bledzki AK, Jaszkiewicz A. Mechanical performance of biocomposites based on PLA and PHBV reinforced with natural fibres - A comparative study to PP. Compos Sci Technol 2010;70:1687–96. https://doi.org/10.1016/j.compscitech.2010.06.005.
[25] Iwatake A, Nogi M, Yano H. Cellulose nanofiber-reinforced polylactic acid. Compos Sci Technol 2008;68:2103–6. https://doi.org/10.1016/j.compscitech.2008.03.006.
[26] Suryanegara L, Nakagaito AN, Yano H. The effect of crystallization of PLA on the thermal and mechanical properties of microfibrillated cellulose-reinforced PLA composites. Compos Sci Technol 2009;69:1187–92. https://doi.org/10.1016/j.compscitech.2009.02.022.
[27] Chen W, Yu H, Liu Y. Preparation of millimeter-long cellulose i nanofibers with diameters of 30-80 nm from bamboo fibers. Carbohydr Polym 2011;86:453–61. https://doi.org/10.1016/j.carbpol.2011.04.061.
[28] Chen W, Yu H, Liu Y, Chen P, Zhang M, Hai Y. Individualization of cellulose nanofibers from wood using high-intensity ultrasonication combined with chemical pretreatments. Carbohydr Polym 2011;83:1804–11. https://doi.org/10.1016/j.carbpol.2010.10.040.
[29] Jofré Barud F, López S, Tapia A, Feresin GE, López ML. Attractant, sexual competitiveness enhancing and toxic activities of the essential oils from Baccharis spartioides and Schinus polygama on Ceratitis capitata Wiedemann. Ind Crops Prod 2014;62:299–304. https://doi.org/10.1016/j.indcrop.2014.08.045.
[30] Wang S, Copeland L. Nature of thermal transitions of native and acid-hydrolysed pea starch: Does gelatinization really happen? Carbohydr Polym 2012;87:1507–14. https://doi.org/10.1016/j.carbpol.2011.09.047.
[31] Grząbka-Zasadzińska A, Klapiszewski Ł, Bula K, Jesionowski T, Borysiak S. Supermolecular structure and nucleation ability of polylactide-based composites with silica/lignin hybrid fillers. J Therm Anal Calorim 2016;126:263–75. https://doi.org/10.1007/s10973-016-5311-3.
[32] Favier V, Canova GR, Cavaillé JY, Chanzy H, Dufresne A, Gauthier C. Nanocomposite

materials from latex and cellulose whiskers. Polym Adv Technol 1995;6:351–5. https://doi.org/10.1002/pat.1995.220060514.

[33] Wang Q, Song H, Pan S, Dong N, Wang X, Sun S. Initial pyrolysis mechanism and product formation of cellulose: An Experimental and Density functional theory(DFT) study. Sci Rep 2020;10:1–18. https://doi.org/10.1038/s41598-020-60095-2.

[34] Hilbers TJ, Wang Z, Pecha B, Westerhof RJM, Kersten SRA, Pelaez-Samaniego MR, et al. Cellulose-Lignin interactions during slow and fast pyrolysis. J Anal Appl Pyrolysis 2015;114:197–207. https://doi.org/10.1016/j.jaap.2015.05.020.

[35] Zhu J, Du C. Interaction between lignin and cellulose during the pyrolysis process. Int J Biol Macromol 2024;265:131093. https://doi.org/10.1016/j.ijbiomac.2024.131093.

[36] Majka TM, Al Nakib R, Menceloglu YZ, Pielichowski K. The Influence of Lignin Derivatives on the Thermal Properties and Flammability of PLA+PET Blends. Materials 2025;18:1–33. https://doi.org/10.3390/ma18174181.

[37] Luo Q, Sun Q, Wu L, Yang Z. Structural characterization of an immunoregulatory polysaccharide from the fruiting bodies of Lepista sordida. Carbohydr Polym 2012;88:820–4. https://doi.org/10.1016/j.carbpol.2011.12.043.

[38] Faruk O, Bledzki AK, Fink HP, Sain M. Biocomposites reinforced with natural fibers: 2000-2010. Prog Polym Sci 2012;37:1552–96. https://doi.org/10.1016/j.progpolymsci.2012.04.003.